SUPPLEMENTARY INFORMATION

Heterozygous mutations in PALB2 cause DNA replication and damage response defects

Jenni Nikkilä[# 1, †], Ann Christin Parplys[# 2], Katri Pylkäs[# 1], Muthiah Bose[1], Yanying Huo[3], Kerstin Borgmann[2], Katrin Rapakko[4], Pentti Nieminen[5], Bing Xia[3], Helmut Pospiech[6,7] & Robert Winqvist[1]

[#]equal contribution

1) Laboratory of Cancer Genetics and Tumor Biology, Department of Clinical Chemistry and Biocenter Oulu, Institute of Diagnostics, University of Oulu, and Oulu University Hospital, 90220 Oulu, Finland.
2) Laboratory of Radiobiology and Experimental Radiation Oncology, University Medical Center Hamburg-Eppendorf, 20246 Hamburg, Germany.
3) Department of Radiation Oncology, Rutgers Cancer Institute of New Jersey and Robert Wood Johnson Medical School, Rutgers, The State University of New Jersey, New Brunswick, NJ 08903, USA.
4) Northern Finland Laboratory Centre NordLab, Oulu University Hospital, and Institute of Diagnostics, University of Oulu, 90220 Oulu, Finland.
5) Medical Informatics and Statistics Research Group, 90014 University of Oulu, Finland.
6) Department of Biochemistry, 90014 University of Oulu, Finland.
7) Leibniz Institute for Age Research – Fritz Lipmann Institute, 07745 Jena, Germany.
[†]Present address: Gene Function Team, Breakthrough Breast Cancer Research Centre, Institute of Cancer Research, London SW3 6JB, United Kingdom.

Correspondence to:

Robert Winqvist, Laboratory of Cancer Genetics and Tumor Biology, Department of Clinical Chemistry and Biocenter Oulu, P.O. Box 5000, 90014 University of Oulu, Finland. TEL: +358-8-3153228, FAX: +358-8-3156354, Email: robert.winqvist@oulu.fi

or

Helmut Pospiech, Department of Biochemistry, P.O. Box 3000, 90014 University of Oulu, Finland, or Leibniz Institute for Age Research – Fritz Lipmann Institute, Beutenbergstr. 11, 07745 Jena, Germany, TEL: +358 294 481151 or +49 3641 656290, FAX: +358-8-5531141, Email: pospiech@fli-leibniz.de

Supplementary Figures S1-S7

Supplementary Tables S1-S3

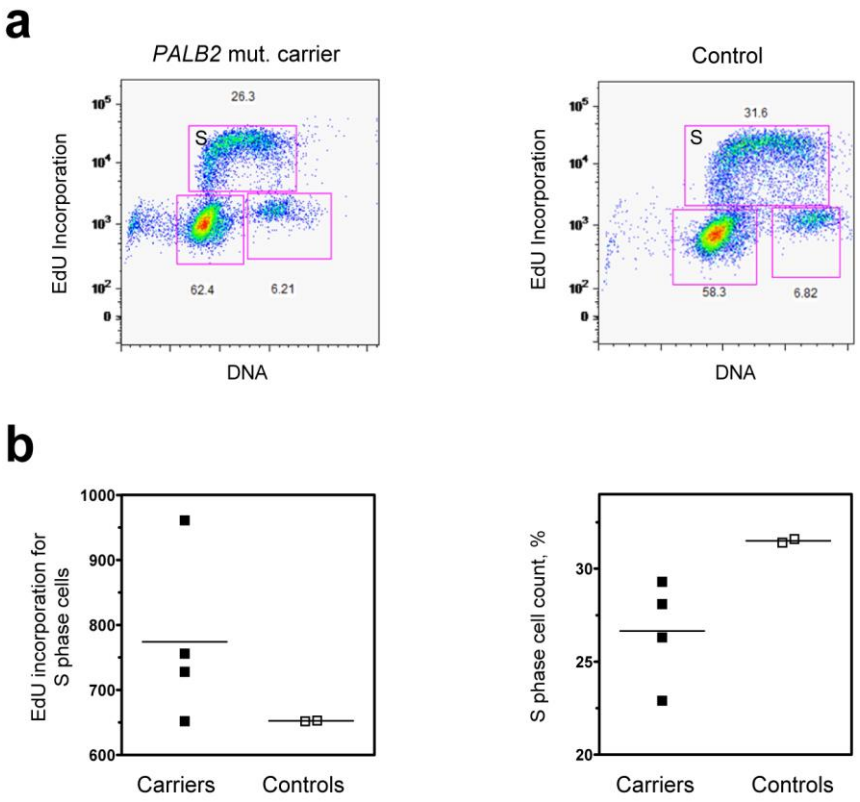

Supplementary Figure S1. *PALB2* mutation carriers show an increase in the DNA synthesis rate and a decrease in S phase cells, when compared to controls. a, Example of the flow cytometric measurement of DNA synthesis rate and S phase cell population. S phase cells were identified after pulse labeling of the cells with EdU and coupling of the EdUMP incorporated with Alexafluor 594 using click chemistry. S phase cells were identified in the AF594 A – DNA405 A dot plot and the mode of the AF594 A signal of the S phase cells were taken as a measure of the DNA synthesis rate. Measurements were done under normal growth conditions, without any toxic treatments. **b,** EdU incorporation showing the active DNA synthesis rates and the percentage of S phase cells. Lines indicate the average of the respective cohorts. Data represents an initial analysis of carrier cell lines BR-0734, BR-0736, BR-0737 and BR-0760, and control cell lines BR-0778 and BR-0781. An independent determination with a larger set of cell lines is presented in Supplementary Table S2.

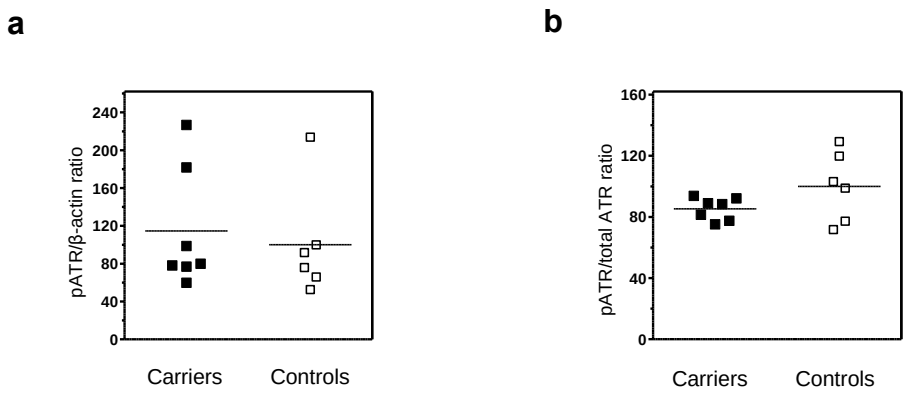

Supplementary Figure S2. Phosphorylation of ATR in untreated cells. a, Comparable levels of ATR phosphorylated at serine 428 in undisturbed *PALB2* c.1592delT mutation carriers and controls, despite the increased levels of total ATR (see **Fig. 4**). **b,** Apparently lower ATR activation by phosphorylation in carrier compared to controls (no statistically significant difference). The level of pATR was related to the total amount of ATR. The data represent the averages of two independent western blot determinations of the same set of samples. Lines indicate the average of the respective cohorts.

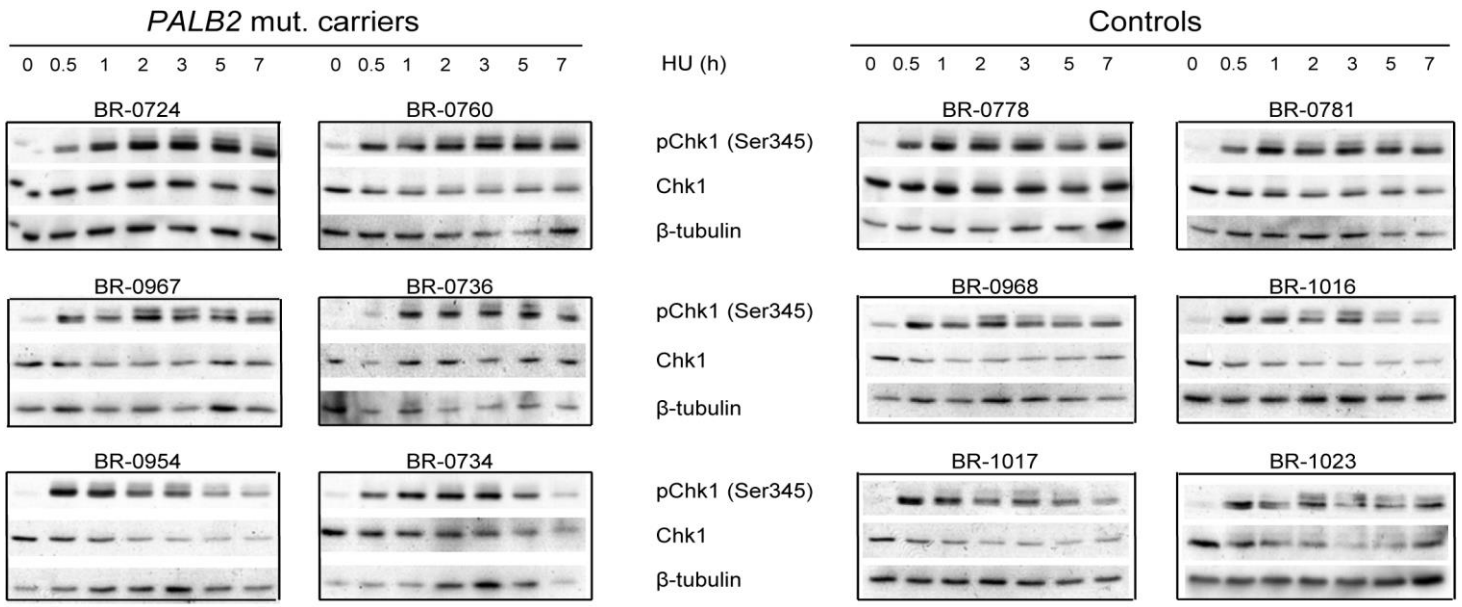

Supplementary Figure S3. Chk1 phosphorylation is delayed in part of the *PALB2* c.1592delT mutation carriers upon replication stress, when compared to controls. Chk1 phosphorylation curves, 0-7 h after HU treatment, were assessed by Western blotting. The bands correspond in all cases to the predicted sizes of 56 kDa [Chk1 and pChk1 (Ser345)] and 50 kDa [β-tubulin]. Positions of the molecular weight markers can be exemplarily inspected in Supplementary Fig. S7 in the full scan of the Immunoblots of Fig. 5.

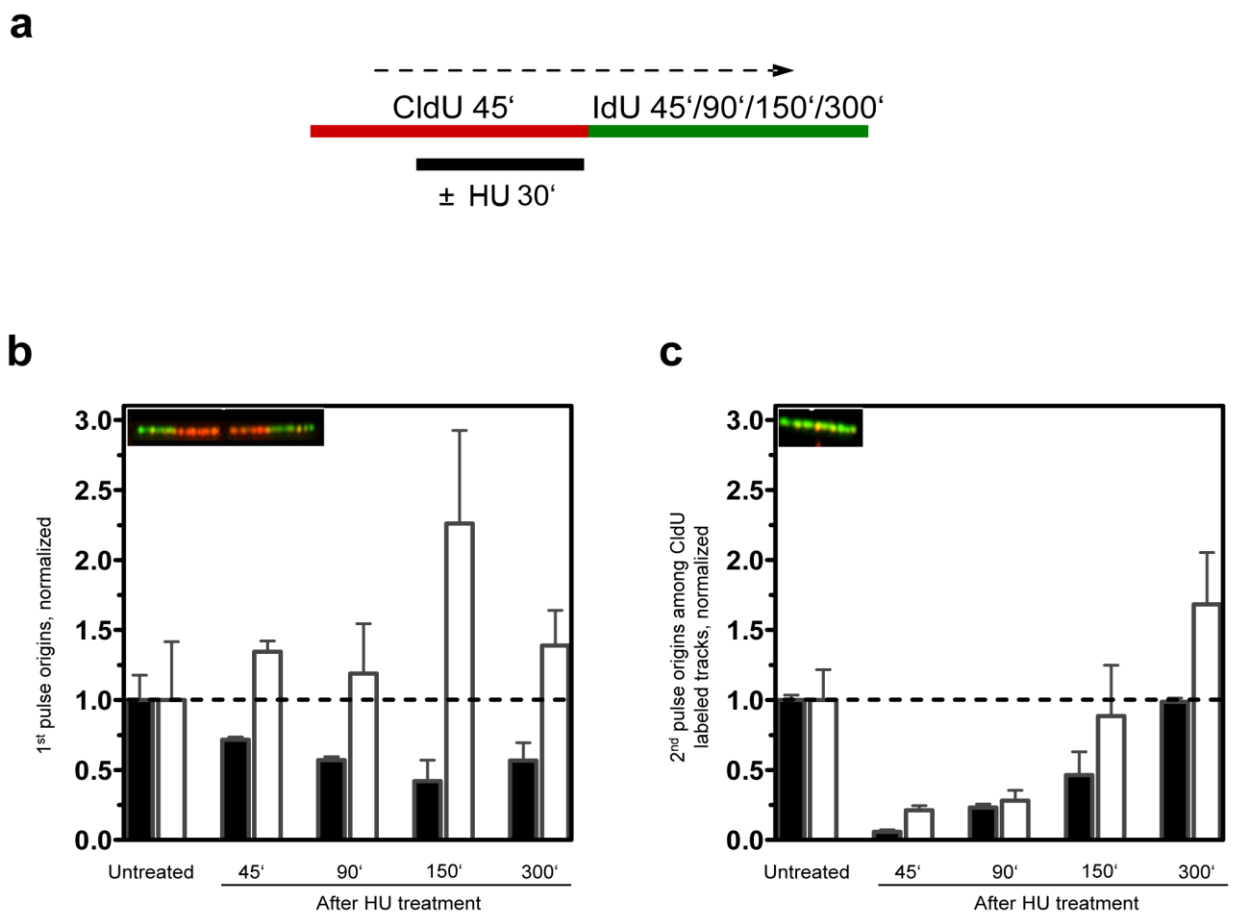

Supplementary Figure S4. Influence of hydroxyurea treatment on DNA replication. a, Labeling protocol for fiber analysis. **b** and **c,** *PALB2* mutation carriers show a decrease in 1st and 2nd pulse origin firing frequency 45, 90, 150 and 300 min after HU treatment. Black bars = carrier, white bars = control. All values were normalized relative to untreated controls. The columns and error bars represent the average and standard deviation of two independent determinations respectively.

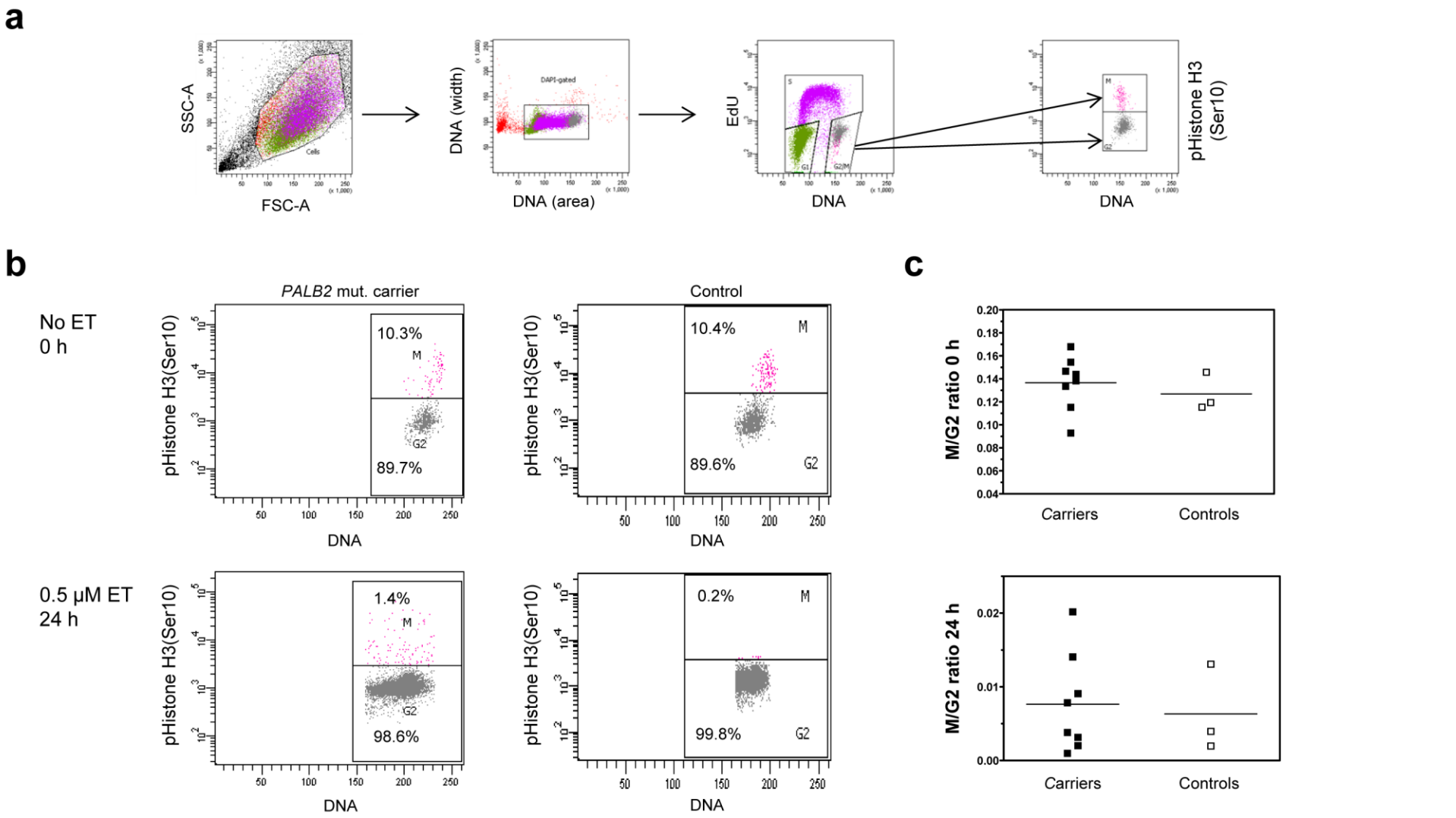

Supplementary Figure S5. Analysis of cell cycle distribution and checkpoint function in lymphoblastoid cell lines. a, The gating and analysis strategy for flow cytometric cell cycle distribution measurements. The cell population was initially gated in a FSC/SSC dot plot and cell duplets were excluded in a DAPI width/DAPI area dot plot, following analysis of the cell cycle distributions by DAPI (DNA content) and EdU

incorporation (DNA synthesis) dot plot to identify G0/G1, S and G2/M phase populations. Finally, mitotic cells were identified within the G2/M phase population as phospho-Histone H3 (Ser10) positives. **b**, Example of a G2/M phase analysis of a *PALB2* mutation carrier and a control cell line, and G2 phase cell numbers and M/G2 ratios before (0 h, top) and 24 h after (bottom) 0.5 µM ET treatment, showing that the control cell line has a tighter G2/M checkpoint than the *PALB2* mutation carrier, apparent as a smaller G2 to M ratio. **c,** Summary of the M/G2 ratio analysis before and after 24 h in the presence of 0.5 µM ET. Lines indicate the average of the respective cohorts. Data points indicate the average of two independent experiments during two separate cultivation periods. For an individual experiment, samples for each cell line were collected at the same time, verifying that cell lines were cultivated the same amount. Although some *PALB2* mutation carrier lines show signs of a compromized G2/M checkpoint, there is no statistically significant difference in the M/G2 ratio between the two cohorts.

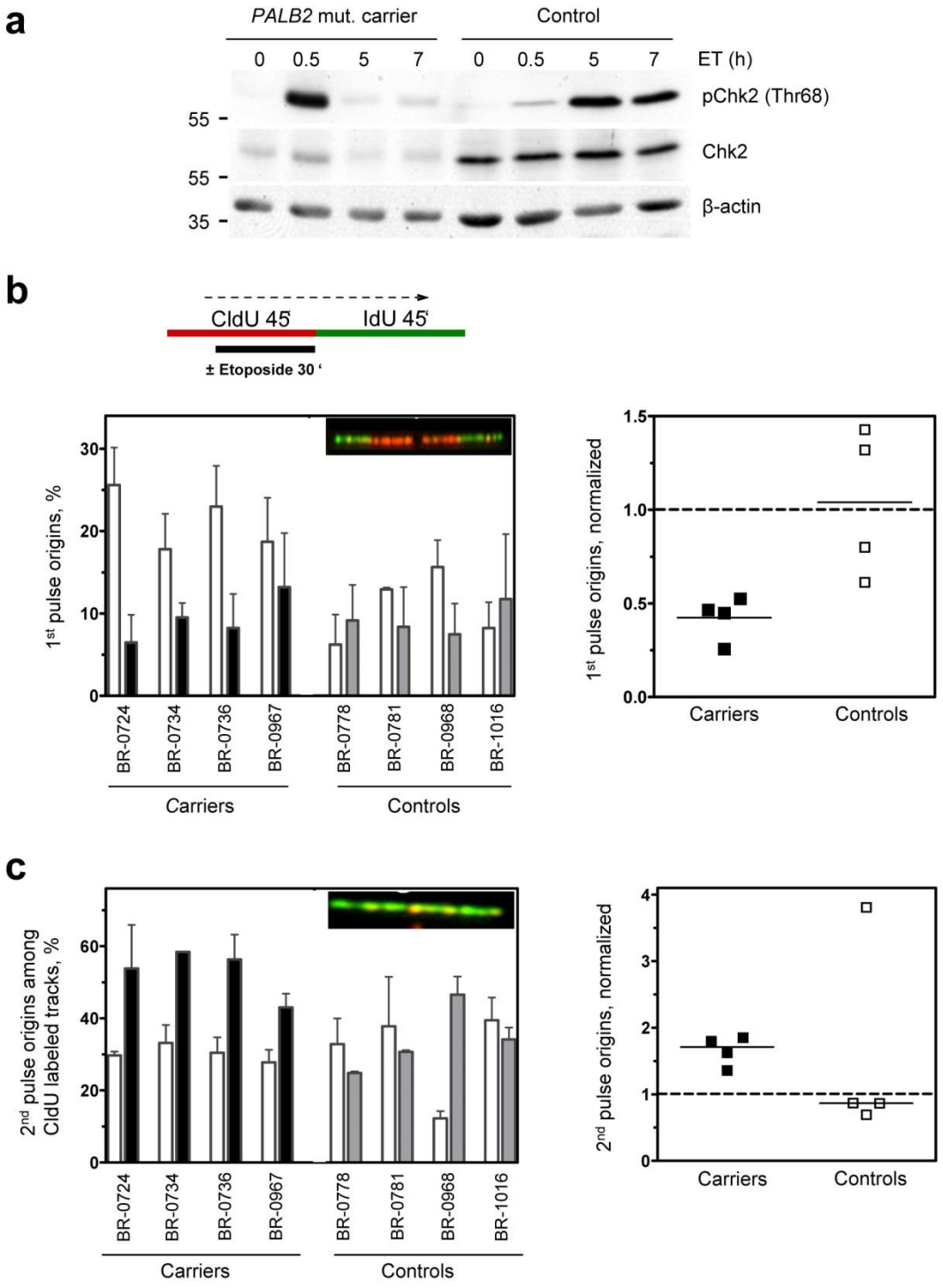

Supplementary Figure S6. Effects of etoposide treatment on Chk2 phosphorylation and DNA replication. a, Western blot analyses of Chk2 phosphorylation time course 0-7 h after ET treatment for one representative *PALB2* mutation carrier and control line, respectively. The predicted size for Chk2/pChk2 is 62 kDa, and levels were normalized against β-actin (42 kDa). **b,** Quantitative fiber assay analysis of 1st pulse origins and **c**, of 2nd pulse origins in untreated carriers and controls after ET treatment. White bars represent untreated mutation carriers and controls. Black and grey bars represent carriers and controls, respectively, after ET treatment. All values presented in panel **b** and **c** represent the average of two independent determinations. The error bars indicate standard deviations. Lines in the dot plots indicate the median of the respective cohorts.

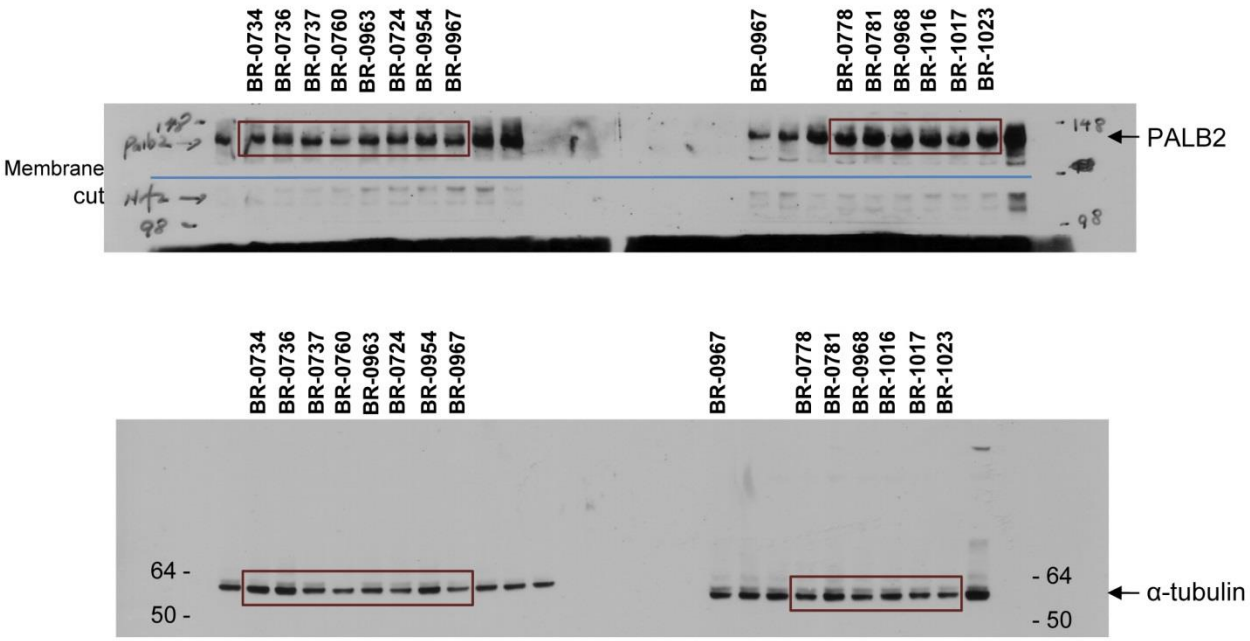

Full scans of the immunoblots of Figure 1a. Blots were acquired by ECL exposure to film.

Supplementary Figure S7. Full Scans of Immunoblots.
Brown rectangles delineate cropped areas used and a blue line indicates cuts in the membrane.

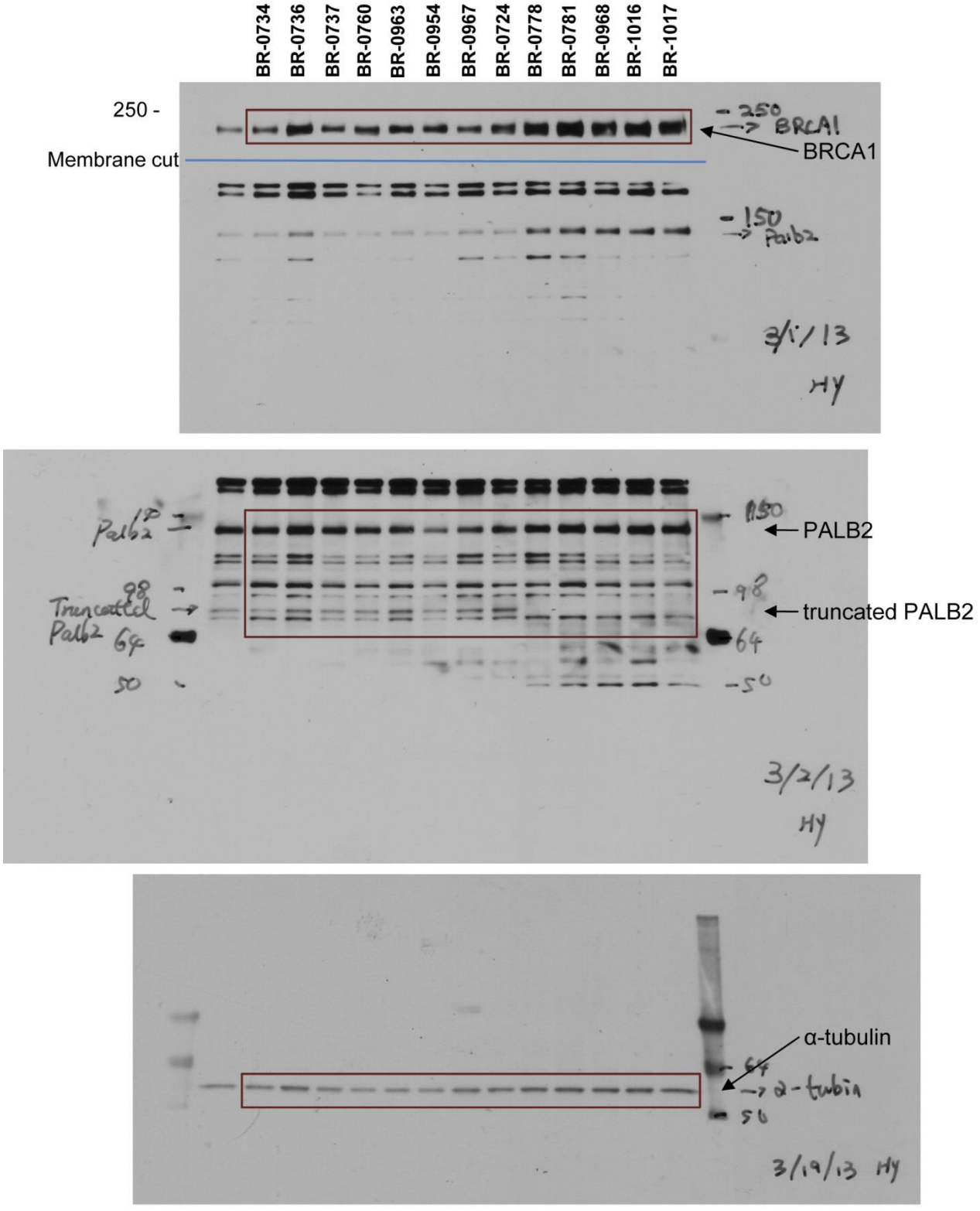

Full scans of the immunoblots of Figure 1b. Blots were acquired by ECL exposure to film.

Supplementary Figure S7 continued.

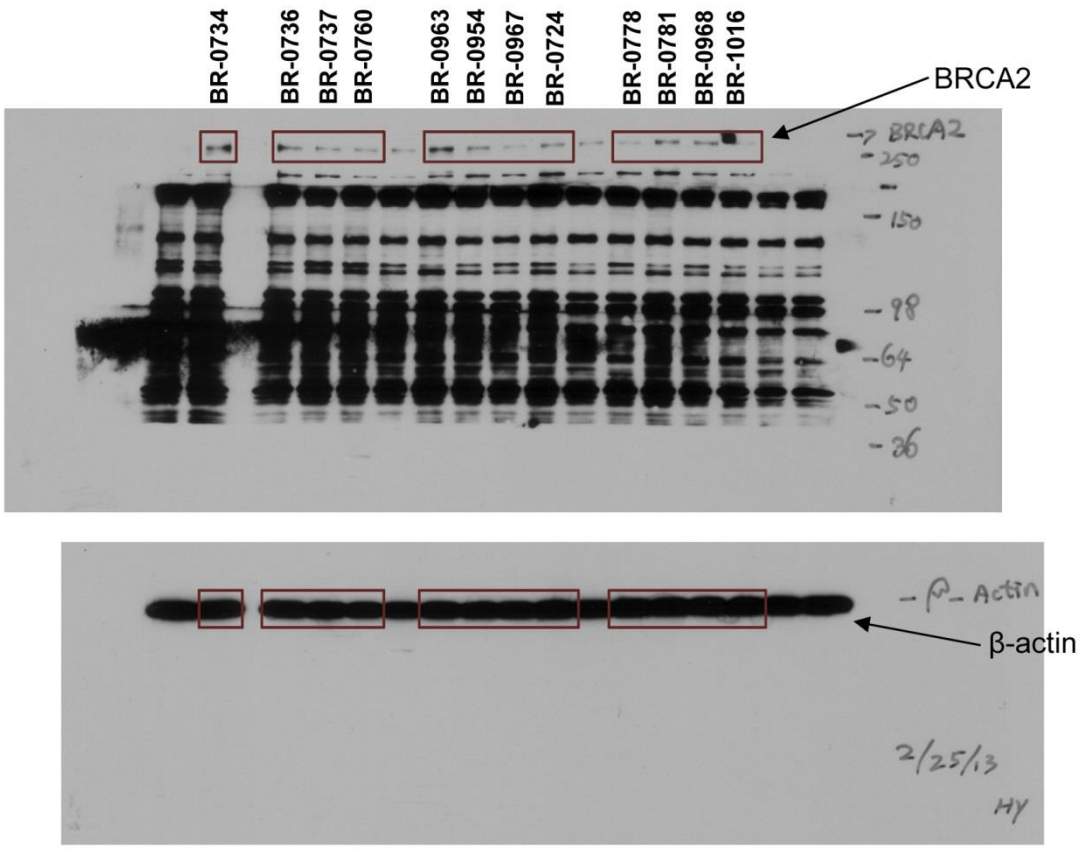

Full scans of the immunoblots of Figure 1c. Blots were acquired by ECL exposure to film.

Supplementary Figure S7 continued.

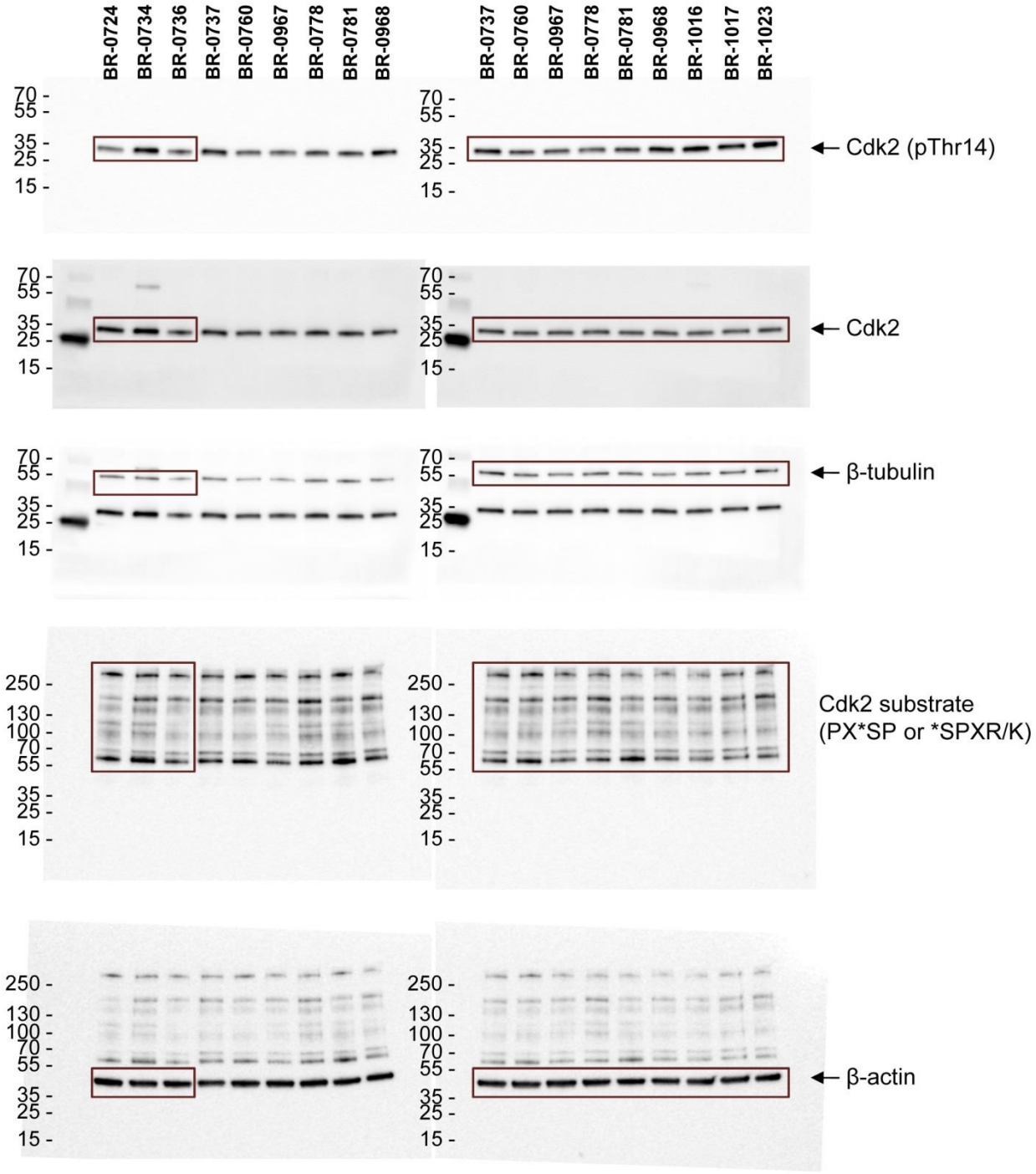

Full scans of the immunoblots of Figure 3. Blots were acquired by ECL and a BioRad Gel Doc EZ System.

Supplementary Figure S7 continued.

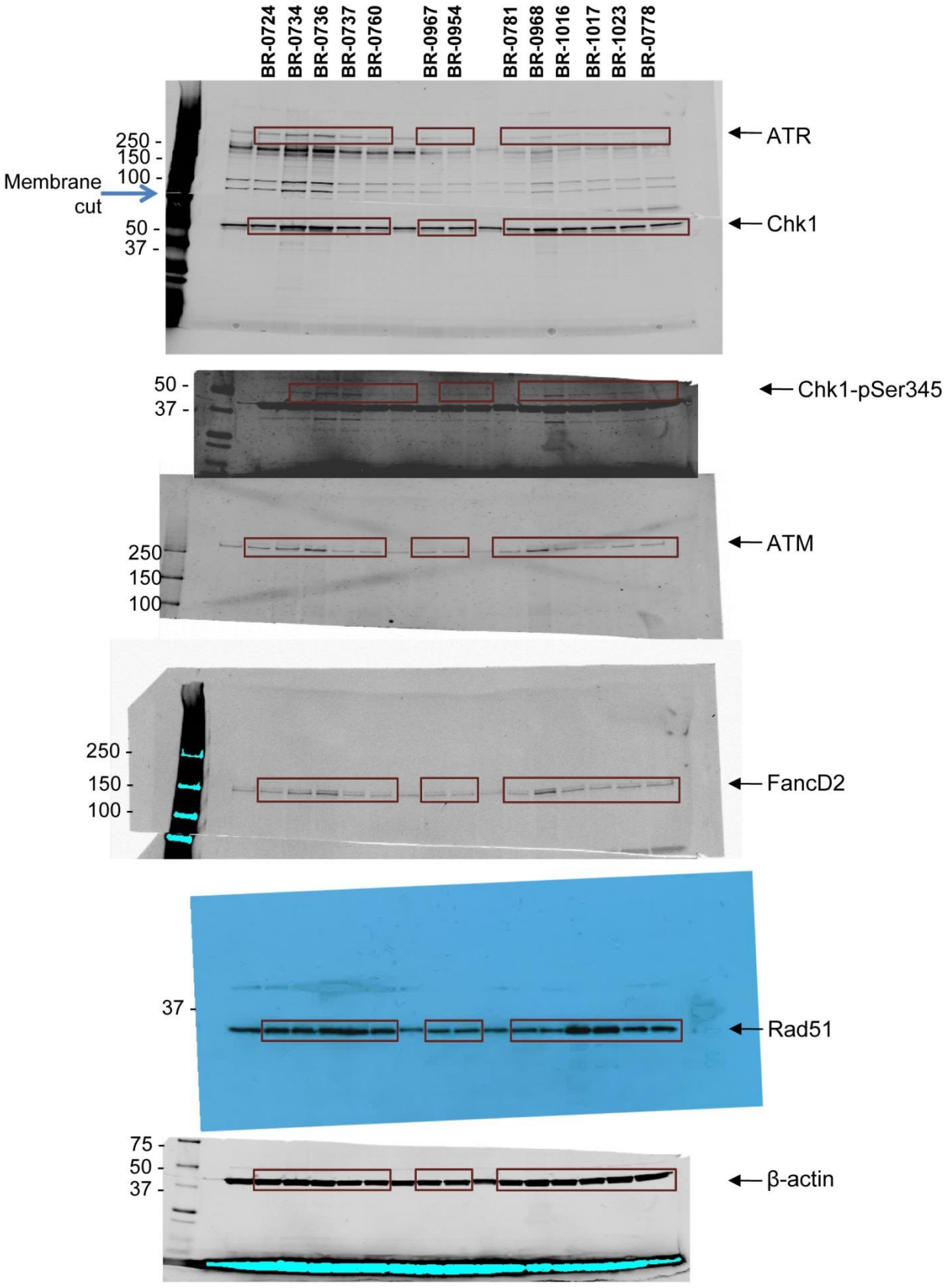

Full scans of the immunoblots of Figure 4. Blots were acquired by Li-Cor Odyssey Infrared Imaging System.

Supplementary Figure S7 continued.

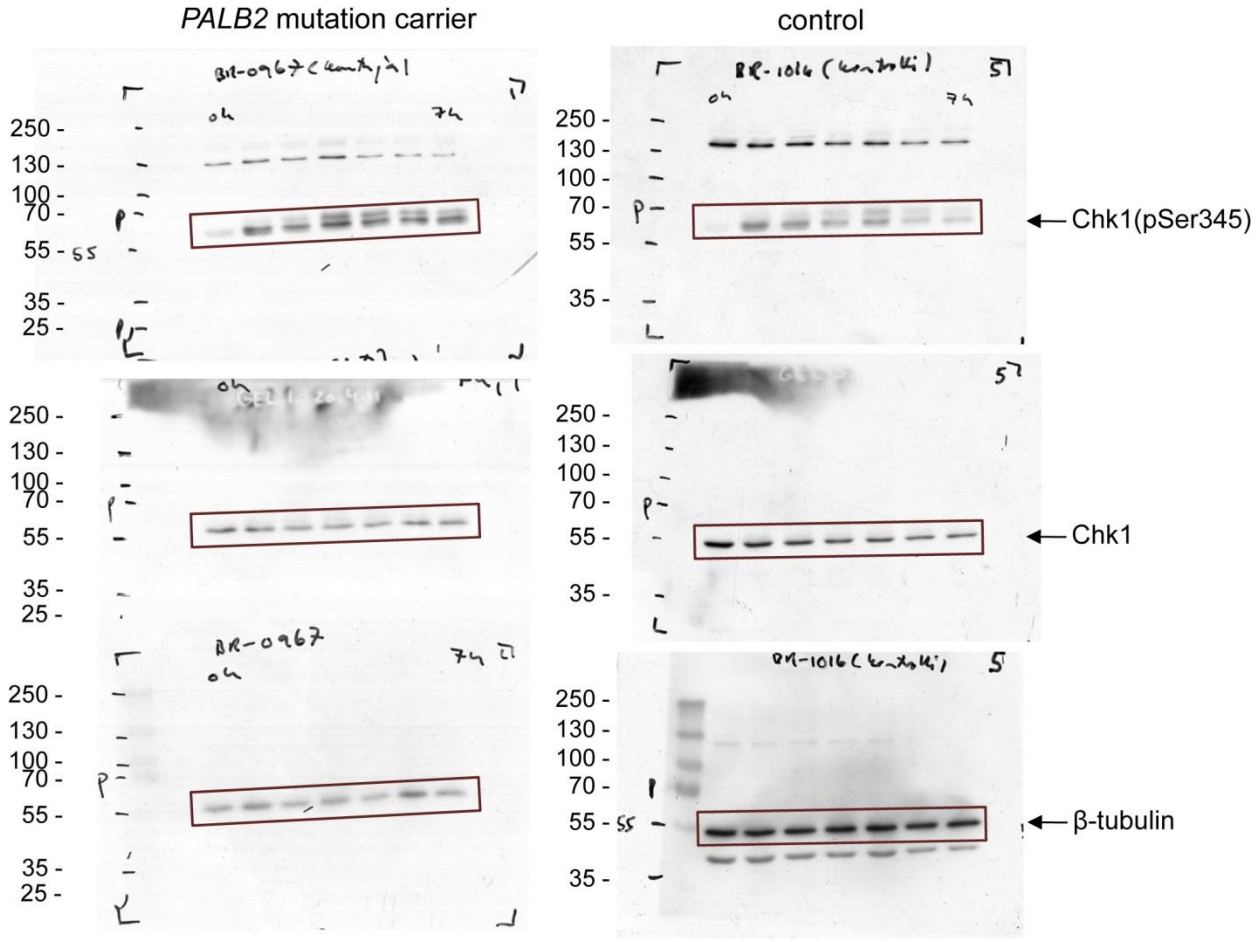

Full scans of the immunoblots of Figure 5. Blots were acquired by ECL and exposure to film.

Supplementary Figure S7 continued.

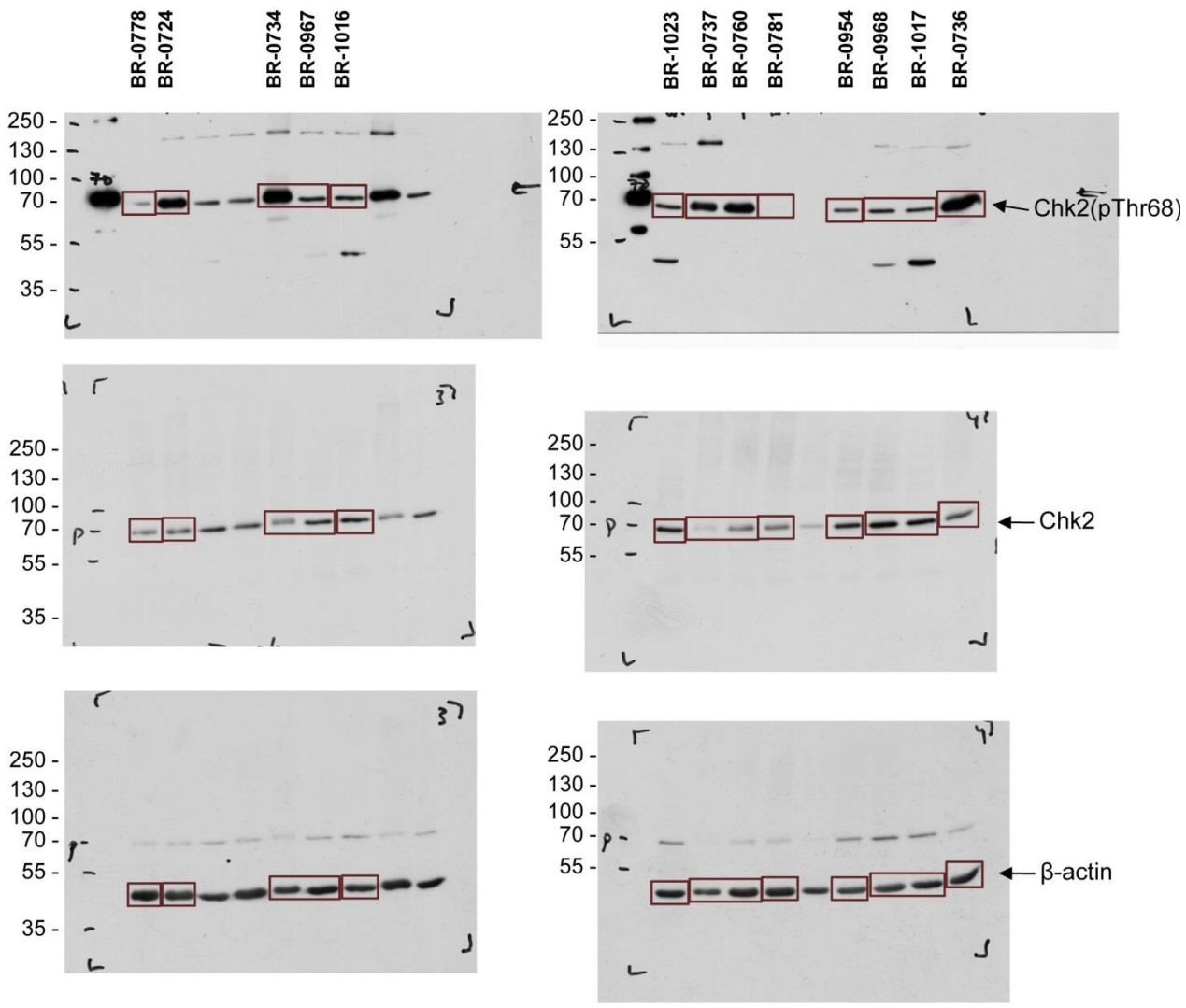

Full scans of the immunoblots of Figure 6a. Blots were acquired by ECL and exposure to film.

Supplementary Figure S7 continued.

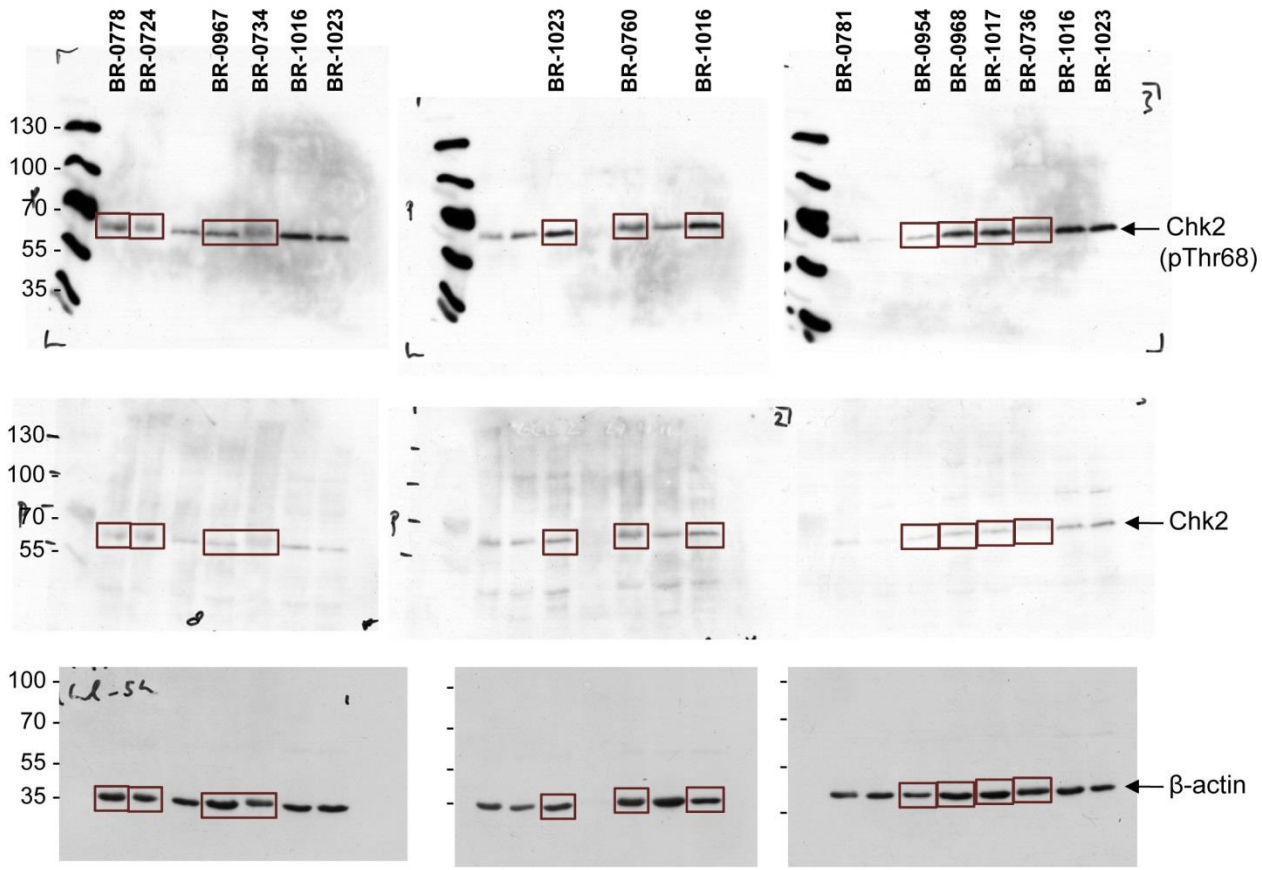

Full scans of the immunoblots of Figure 6b. Blots were acquired by ECL and film exposure

Supplementary Figure S7 continued.

Supplementary Table S1. Studied lymphoblastoid cell lines.

Cell line	Health status	Age at breast cancer diagnosis or disease monitoring (y)	Mutational status	Relationship
BR-0724	Patient	56	*PALB2* c.1592delT	-
BR-0734	Patient	64	*PALB2* c.1592delT	-
BR-0736	Patient	49	*PALB2* c.1592delT	-
BR-0737	Patient	62	*PALB2* c.1592delT	-
BR-0760	Patient	49	*PALB2* c.1592delT	-
BR-0963	Patient	60	*PALB2* c.1592delT	-
BR-0778	Healthy	49	-	-
BR-0781	Healthy	44	-	-
BR-0954	Healthy	23	*PALB2* c.1592delT	Patient´s BR-0760 daughter
BR-0967	Healthy	44	*PALB2* c.1592delT	Patient´s BR-0737 daughter
BR-0968	Healthy	50	-	Patient´s BR-0737 daughter
BR-1016	Healthy	53	-	-
BR-1017	Healthy	56	-	-
BR-1023	Healthy	65	-	-

Supplementary Table S2. Cell cycle distribution of lymphoblastoid cell lines after 0.5 µM ET treatment.

0 h = without etoposide treatment.

Cell line	G1/G0			S phase			G2 phase			M phase		
	0 h	6 h	24 h	0 h	6 h	24 h	0 h	6 h	24 h	0 h	6 h	24 h
PALB2 mut. carriers												
BR-0724	65.75	61.60	55.90	29.90	28.50	16.95	3.85	9.70	27.09	0.51	0.13	0.13
BR-0734	64.70	64.10	64.30	28.60	26.80	10.60	5.92	8.97	25.42	0.79	0.13	0.08
BR-0736	57.30	52.80	38.90	39.70	41.10	30.60	2.69	6.03	30.60	0.31	0.07	0.43
BR-0737	62.40	57.30	48.30	29.80	28.80	10.80	6.82	13.70	40.90	1.00	0.00	0.04
BR-0760	74.20	73.20	69.10	20.40	18.20	13.40	4.95	8.39	17.64	0.46	0.13	0.16
BR-0954	51.70	47.40	54.90	43.90	40.00	25.10	3.82	12.51	20.44	0.59	0.09	0.16
BR-0967	56.90	53.10	49.60	38.90	36.30	29.40	3.69	10.69	21.02	0.51	0.01	0.08
Controls												
BR-0778	63.70	56.70	52.20	30.80	29.60	26.90	4.85	13.80	20.26	0.56	0.00	0.04
BR-0781	64.10	65.40	55.20	28.70	24.60	14.40	6.45	10.00	30.31	0.77	0.10	0.12
BR-0968	54.40	49.70	56.10	41.50	42.20	28.60	3.50	8.22	15.30	0.51	0.10	0.20

Supplementary Table S3. Primary and secondary antibodies used in Western blot and fiber assays.

Target	Clone	Species	Reference
β-actin	AC-15	Mouse monoclonal	Sigma-Aldrich
ATM	D2E2	Rabbit monoclonal	Cell Signaling Technology
ATR	2B5	Mouse monoclonal	Abcam
Phospho-ATR (Ser428)	-	Rabbit polyclonal	Cell Signaling Technology
BRCA1	07-434	Rabbit polyclonal	Merck Millipore
BRCA2	Ab-1	Mouse monoclonal	Merck Millipore
Anti-BrdU	BU 1/75	Rat monoclonal	AbD Serotec
Anti-BrdU	B44	Mouse monoclonal	Becton Dickinson
Cdk2	Sc-163	Rabbit polyclonal	Santa Cruz Biotechnology
Phopho-Cdk2 (Thr14)	EP2234Y	Rabbit monoclonal	Abcam
Chk1	G4	Mouse monoclonal	Santa Cruz Biotechnology
Chk1	2G1D5	Mouse monoclonal	Cell Signaling Technology
Phospho-Chk1 (Ser345)	133D3	Rabbit monoclonal	Cell Signaling Technology
Chk2	7	Mouse monoclonal	Merck Millipore
Phospho-Chk2 (Thr68)	-	Rabbit polyclonal	Cell Signaling Technology
FANCD2	FI17	Mouse monoclonal	Santa Cruz Biotechnology
Phospho-MAPK/CDK substrates (PXS*P or S*PXR/K)	34B2	Rabbit monoclonal	Cell Signaling
PALB2		Rabbit polyclonal	Raised against aa 1-120 mapping in N-terminal PALB2
RAD51	3F326	Mouse monoclonal	biomol
α-tubulin	GTX102078	Rabbit polyclonal	GeneTex
β-tubulin	KMX-1	Mouse monoclonal	Merck Millipore
Goat anti-mouse IRDYE® 680		Goat polyclonal	LI-COR Bioscience
Goat anti-rabbit IRDYE® 800 CW		Goat polyclonal	LI-COR Bioscience
Goat anti-mouse IRDYE® 800 CW		Goat polyclonal	LI-COR Bioscience
Goat anti-rabbit IRDYE® 680		Goat polyclonal	LI-COR Bioscience
Anti-Rat Alexa Fluor 555		Goat polyclonal	Molecular Probes
Anti-Mouse Alexa Fluor 488		Goat polyclonal	Molecular Probes
AP-conjugated goat anti-rabbit IgG		Goat polyclonal	Jackson ImmunoResearch
HP-conjugated goat anti-rabbit IgG		Goat polyclonal	Jackson ImmunoResearch
HP-conjugated goat anti-mouse IgG		Goat polyclonal	Jackson ImmunoResearch

AP = alkaline phosphatase.

HP = horseradish peroxidase.